Heat Transfer in Plasma-Arc Welding

In comparing plasma and gas tungsten welding arcs, significant differences are found in heat transfer distribution and efficiency

BY J. C. METCALFE AND M. B. C. QUIGLEY

ABSTRACT. The processes by which heat is transferred to the workpiece are examined for a 10 kW plasma welding arc. A comparison is made with a 1.6 kW gas tungsten-arc. Both keyhole (fully penetrated) and unpenetrated welds are considered. The (averaged) arc temperature can be deduced from the enthalpy flow in the plasma. In plasma welding the heat transfer by convection is an important process, by which 27 to 31% of the total power input to the arc (VI) is transferred to the workpiece. It is also shown that radiation can account for 17 to 19% of the total power input being transferred to the weld.

Thus in plasma-arc welding, unlike gas tungsten-arc welding, convection and radiation are the dominant processes with the contribution from anode effects somewhat smaller. It is shown that in a 10 kW argon plasma welding arc an efficiency of heat transfer to the anode of 60 to 66% is to be expected.

Introduction

The heat flow to the workpiece in gas tungsten-arc welding has been examined previously (Ref. 1). Then it was shown that in a 100 A, 16 V gas tungsten-arc only 5% (less than 100 W) of the total arc power (VI) is transferred to the workpiece by convection, conduction and radiation. The majority (39%, 630 W) is due to the surface effects at the anode.

The arc used in plasma arc welding (PAW) is significantly different from a gas tungsten-arc. It is constricted by a small nozzle (typically 3 mm diam) and has a much higher gas velocity and temperature as shown in Table 1. The high gas velocities associated with plasma arc welding have two important consequences.

The momentum of the gas stream causes a deformation in the weld pool surface and this can be developed to form a 'keyhole' in the weld (Figs. 1 and 2). In this mode of operation a hole is formed completely through the base metal. As the torch moves along the weld, the metal which is melted in advance of the keyhole resolidifies at the rear to form the weld bead. Although "keyholing" began as a gas welding technique, it is seldom used in this manner today. Keyholes are also formed in electron beam and laser welding, although in these cases they are produced mainly by the pressure of the evaporating metal and call for power densities above 10 GW/m^2.

The proportion of the total arc power (VI) transferred by convection to the workpiece is likely to be much higher for the plasma welding arc than for the gas tungsten-arc.

In this paper an examination is made of the energy transfer to the workpiece with a plasma welding arc. The relative contributions from radiation, convection and electron effects at the anode will be compared with those for the GTAW process. Averaged values for arc temperature and emissivity have been deduced and await experimental verification.

An assessment of the power input processes within a plasma welding

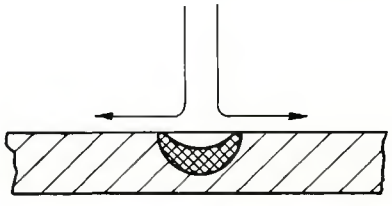

Fig. 1 — Gas flow impinging on surface of weld pool before keyhole is produced

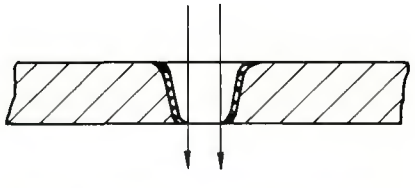

Fig. 2 — Gas flow through keyhole

Table 1 — Comparison of Plasma Arc and Gas Tungsten-Arc Welding

	GTAW	PAW
Gas velocity, m/s	80 – 150	300 – 2000
Arc temperature, K	8000 – 15000	10000 – 20000
Power density, MW/m^2	10 – 100	100 – 10000

The authors are associated with the Central Electricity Generating Board, Marchwood Engineering Laboratories, Marchwood, Southampton, Hants, United Kingdom.

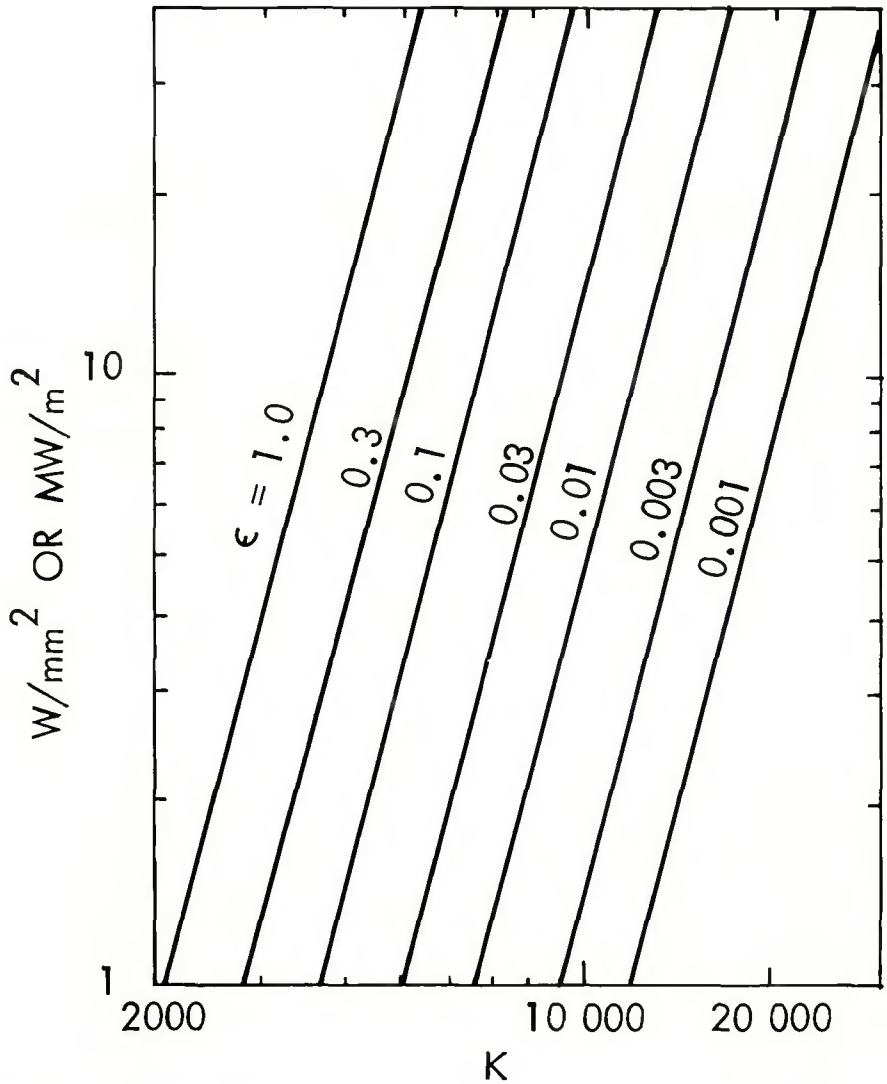

Fig. 3 — Radiation loss

arc should help future investigations into the effect of variation of the welding parameters, such as gas flow, current, etc. on the depth of penetration of the weld. Although plasma arc welding is possible with a non-transferred arc, this mode (which is usually reserved for working non-conducting materials) will not be considered here.

PAW Properties and Power Flow

Typical dimensions and possible process settings are shown in Table 2.

The values in Table 2 are based on experimental experience and represent reasonable mean values. For the purpose of these calculations it is assumed that the arc temperature is uniform. In practice this will be fairly valid across the core (Refs. 2, 3) but less so in outer regions.

Electron Effects at the Anode ($P_{el.}$)

Work Function (ϕ) — The potential energy given up to an anode by an electron entering the surface corresponds to the work function of the metal. For the applications considered here the metal anode, either at the plane surface or inside the keyhole, is of steel. The value of ϕ for iron is in the range 4.0 to 4.5 V but the actual value of ϕ will depend upon what other constituents are being used in the steel (Mn for example has ϕ = 3.8 V). As in Quigley et al (Ref. 1) we will choose a mean value for ϕ of 4.2 V giving, at 250 A, an energy dissipation at the anode of 1050 W.

Anode Fall (V_a) — In normal circumstances the anode does not emit positive ions so that the current to the surface is carried solely by electrons. There will therefore be an excess of negative space charge near the anode with a corresponding potential drop, the anode fall. The magnitude of this fall is determined to a certain extent by the vapor conditions at the surface. If there is intense vaporization, then it is relatively easy to generate positive ions (the ionization potential for Fe is 7.8 V). However, if there is no vaporization, the anode fall has to be sufficiently great for the electrons in the high energy tail of the electron energy distribution to ionize argon (at 15.6 V), i.e., a mean energy of a few eV.

Table 2 — Dimensions and Process Settings

Diameter of arc:	
At nozzle, mm	2.5
Near weld, mm	6.0
Length of arc, mm	5.0
Diameter of weld pool, mm	8.0
Diameter of keyhole:	
At top, mm	6.0
At bottom, mm	2.0
Depth of keyhole, mm	6.0
Gas flow:	
m′, g/s	0.22
v'_0, cfh	16.0
Arc current (I), A	250.0
Arc voltage (V), V	40.0

In our case the pool temperatures are almost certainly high enough for considerable vaporization to occur. The paper by Milner et al (Ref. 4) suggests that a low value of anode fall should be taken. Recent work (Ref. 5) confirms this and puts the anode fall between 0 and 2 V. A figure of 1 V is therefore taken for anode fall in the plasma welding situation. It is questionable whether the anode fall would be the same in both the blunt-plate and the keyhole geometry, but since, as yet, there is no firm evidence to suggest otherwise, they will be considered equal in this paper.

Electron Thermal Energy — The problem here is to estimate the electron temperature near to the anode.

The temperature in the bulk of the plasma (argon) may be 15000 K or more, whereas the vapor temperature at the surface will be of order 3000 K. The mean of these two temperatures (9000 K) is taken here as the best estimate of the relevant electron temperature, so that P = (3kT/2e)I = 270 W (k is Boltzmann's constant).

It should be borne in mind that the temperature of the bulk of the plasma will be determined later, using these previously calculated anode losses. Strictly speaking iterative procedures should, therefore, be used to give a more precise evaluation but at this stage the temperature is not critical as the electron thermal energy is small relative to the other energy dissipation processes.

The summation of the heat released at the workpiece due to anode effects is therefore

$$P_{el.} = 1050 + 250 + 270 \text{ W} = 1570 \text{ W}$$

Enthalpy Flow and Temperature in the Arc

To calculate the heat transfer by convection it is necessary to know the temperature of the arc column. At present there are no experimental

measurements or analytical studies available which give the temperature distribution across this type of welding arc. In these circumstances one approach is to find an average temperature (T_a) across the arc and this is done here. It is, of course, recognized that this approach has limitations. The temperature may be deduced from the total enthalpy flow in the arc (i.e. the energy transported past any cross-section of the arc)

$$m'H = VI - \text{electrode effects} - \text{radiation losses}$$

The losses at the cathode (i.e. that heat which is conducted away and does not enter the arc) are small, typically 2% of the total power input, VI (Ref. 6).

The radiation losses (radial) were taken to be 20% of VI (Refs. 2, 7), i.e., 2 kW. Hence

$$m'H = 9800 - 1570 - 2000 = 6230 \text{ W}$$

and thus

$$H = 27.9 \text{ MJ/kg}$$

From Table 3 it can be seen that this enthalpy corresponds to a temperature of 14200 K approximately, hence T_a = 14200 K.

Table 3 — Properties of Argon at 1 Atmosphere (from Refs. 12 and 13)

Temperature, K	Enthalpy, H, MJ/kg	Specific heat, C_P, kJ/kg K	Density, ρ, g/m³	Viscosity, μ, mg/m s	Thermal conduct'y, k, W/m K	Speed of sound, c, km/s	Rates of specific heats, c_P/c_V
5000	2.600	0.519	97.32	148	0.12	1.317	1.67
6000	3.127	0.519	81.10	173	0.21	1.443	1.67
7000	3.651	0.540	69.50	193	0.36	1.542	1.63
8000	4.228	0.628	60.73	207	0.58	1.594	1.53
9000	4.965	0.892	53.72	218	0.91	1.605	1.38
10000	6.124	1.511	47.68	225	1.35	1.628	1.27
11000	8.184	2.721	41.98	218	1.95	1.695	1.25
12000	11.83	4.676	36.23	200	2.70	1.814	1.32
13000	17.78	7.242	30.39	175	3.60	1.980	1.45
14000	26.12	9.251	24.92	147	4.25	2.182	1.63
15000	35.53	9.251	20.54	119	4.15	2.404	1.85
16000	43.83	7.158	17.52	96	3.70	2.622	2.06
17000	49.77	4.730	15.55	75	3.20	2.838	2.28
18000	53.71	3.211	14.22	58	2.78	3.047	2.48
19000	56.59	2.733	13.25	45	2.43	3.146	2.50
20000	59.44	3.135	11.24	35	2.12	3.188	2.44
21000	63.12	4.425	11.62	27	2.03	3.215	2.36
22000	68.61	6.572	10.85	21	2.07	3.283	2.35
23000	76.44	9.084	10.04	16	2.20	3.394	2.41
24000	86.65	11.218	9.22	15	2.42	3.537	2.50
25000	98.37	12.098	8.436	17	2.75	3.702	2.63

Radiation

Radiation from the Arc — The power radiated by the arc is given by

$$P_{ra} = 0.057 \varepsilon A(T_a/1000)^4 \text{ MW}$$

where T_a is temperature, A is the surface area and ε is the emissivity of the arc. Values of the surface power density (P_{ra}/A) are plotted in Fig. 3 as a function of arc temperature and emissivity.

The main problem in calculating radiation from the arc is the selection of the correct value for emissivity. The Welding Handbook (Ref. 2) suggested that up to 20% and Emmons (Ref. 7) found that up to 25% of the total power (VI) in high temperature welding arcs is lost by radiation. If 20% is taken for the arc considered here (10 kW total power input) then the power lost radially from the surface of the arc column (70 mm²) is 2 kW. From this assumption and using the mean arc temperature derived earlier of 14200 K the emissivity is found to be 0.012. At this stage it is suggested that this is the most appropriate value for ε but this will need verification.

Radiation to the Weld — Assuming that the emissivity of the arc towards the weld is the same as that applying radially, i.e., ε = 0.012 and that the absorbtivity of the weld is η then the power input to the workpiece by radiation from the arc is:

1. To the weld pool assuming a surface area under the deflected arc of A = 113 mm² and that the mean temperature of 14200 K still applies

$$P_{r,w} = 3.47\eta \text{ kW}$$

2. To the keyhole with a surface area of 79 mm²

$$P_{r,w} = 2.4\eta \text{ kW}$$

For the flat plate weld pool η will be about 0.5 but for the keyhole the radiation will be partially trapped; i.e., it is an almost perfect absorbing cone, so that we will take η = 0.8. Therefore

$P_{r,w}$ (weld pool) = 1.74 kW

and $P_{r,w}$ (keyhole = 1.92 kW

Gas Velocity

In the tungsten arc the velocity of the shielding gas issuing from the torch nozzle is negligible. In the arc column, velocities of up to 120 m/s have been predicted (Ref. 1) due to the difference in magnetic pressure between different points along the arc.

In the plasma welding arc considered here the gas velocity can be deduced from the known dimensions and mass flow in the system. Assuming that there is no entrainment of shielding gas and that all the gas issuing from the central nozzle of the torch remains within the arc boundary, then

$$\rho vA = m' = \rho_o v'_o$$

where A is the cross-sectional area of the arc and ρ_o and v'_o are the density and volume flow rates at s.t.p. Usually v'_o is adopted as the process setting; it is typically 16 cfh but can lie anywhere in the range 5 to 20 cfh (0.07 to 0.28 g/s).

The gas velocity near to the weld can be so calculated for the present arc (T_a = 14200 K, d = 6 mm, v'_o = 0.45 m³/h) to give v = 323m/s.

Power Transfer by Convection

The power transferred to the workpiece by convection from the arc can be written as

$$P_{cv} = h \delta H A$$

where A is the surface area on which the arc impinges, δH is the enthalpy difference between the fluid at the temperature of the solid and that at the temperature of the bulk of the fluid and h is so defined as the heat transfer coefficient for the process. It can be shown from a consideration of fluid dynamics (Refs. 8,9 and 10) that

$$Nu = B\, Re^m Pr^n$$

where the non-dimensional parameters are defined as

Nu (Nusselt number) = hdc_P/κ

Re (Reynolds number) = $\rho vd/\mu$

Pr (Prandtl number) = $c_P\mu/\kappa$

and

c_P = specific heat of fluid

d = characteristic dimension for the flow

κ = thermal conductivity of fluid

v = flow velocity

ρ = density of fluid

μ = viscosity of fluid

The constants B, m and n are determined empirically for the particular geometry of the flow under consideration. Hence

$$P_{cv} = A\kappa\, Nu\, \delta H/d\, c_P = A\kappa\, B\, Re^m Pr^n \delta H/d\, c_P$$

Schoeck (Ref. 11) suggests that the

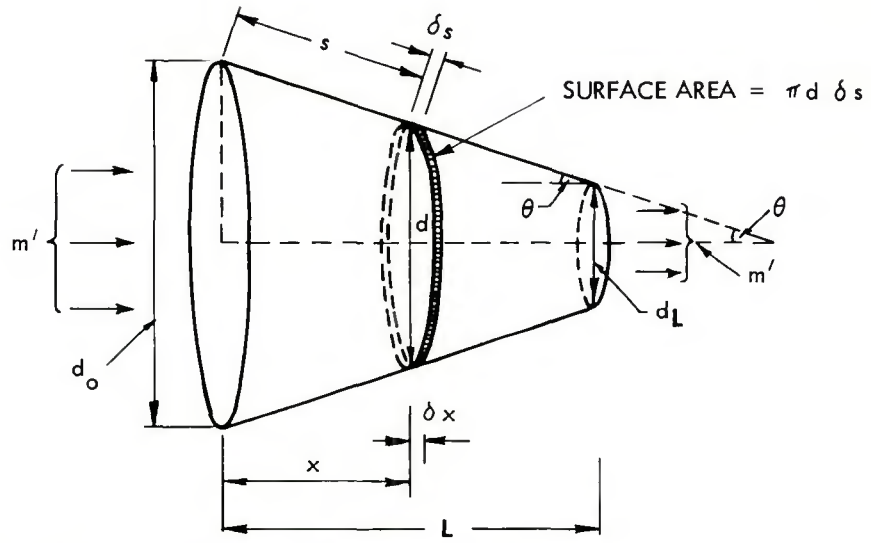

Fig. 4 — Section through model for keyhole

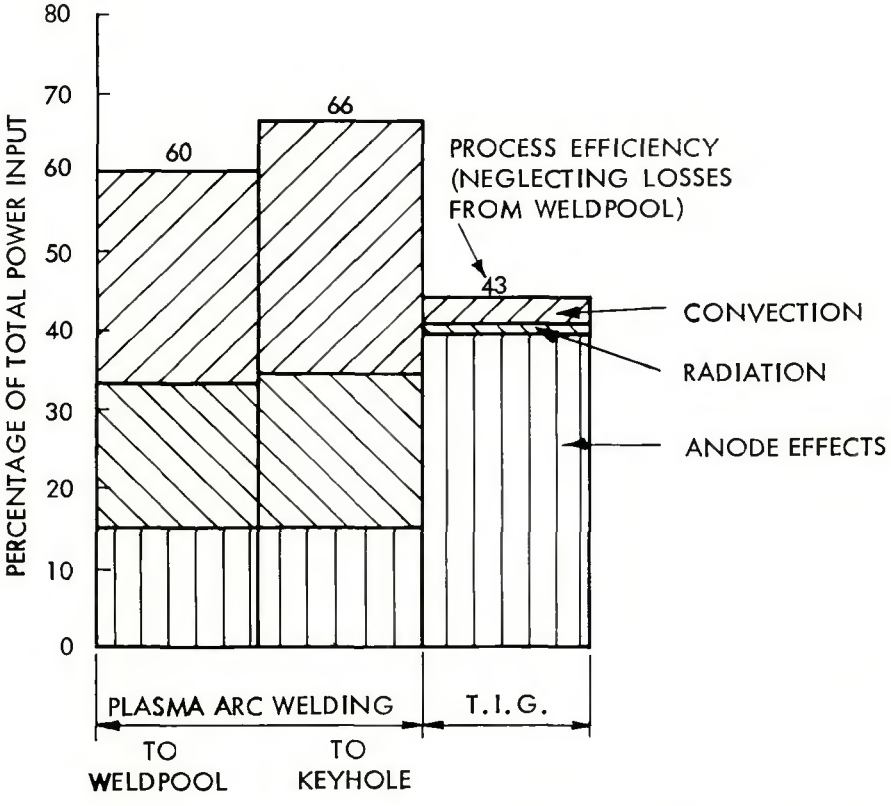

Fig. 5 — Comparison of relative magnitudes of power transfer processes for a 10 kW plasma and a 1.6 kW gas tungsten welding arc.

parameters Re, Pr and Nu should be calculated using gas properties corresponding to a temperature (T_m) at which the enthalpy of the gas is equal to the mean of its enthalpy at the temperature of the arc and of the weld pool

$$H(T_m) = (H_a + H_w)/2$$

In plasma welding there are two characteristic geometries which are of relevance. Initially, before a keyhole is formed, there will be a gas flow impinging perpendicularly on the surface of the weld pool and being deflected across the weld surface radially away from the stagnation point (Fig. 1). Once a keyhole is produced a significant proportion of the gas flow will pass through the workpiece to be discharged on the underside of the weld (Fig. 2). It is suggested that these two situations should be treated separately.

Convective Power Transfer to the Weld Pool — The quoted values for m and n for the flat plate (weld pool) condition are 0.5 and 0.33 respectively (Ref. 9). Values for B are quoted as 0.76 by Eckert & Pfender (Ref. 9) and 0.8 by Wilkinson & Milner (Ref. 10). The latter authors estimated that there could be errors of up to 40% in their value for B due to the dramatic radial variation in the heat transfer coefficient. For example they quote a factor of 2.5 to 3 between the higher coefficient for the heat transfer around the stagnation point and that further out where the flow is parallel to the surface. (This is an agreement with Rogers & Mayhew (Ref. 8, p. 485) who quote B = 0.332 for flow across a flat plate).

Using the arc temperature calculated previously from the total enthalpy flow in the arc (T_a), the power input by convection to the anode, taken within a distance from the stagnation point equal to the diameter of the jet (Ref. 10), so that the area of impingement has a diameter of 12 mm, can be calculated as follows:

$$H_a = 27.9 \text{ MJ/kg};$$
$$H_w = 1.42 \text{ MJ/kg}$$

Therefore H_m = 14.7 MJ/kg which corresponds to a temperature T_m 12500 K and this is the temperature at which the gas properties should be taken in deriving the Reynolds, Prandtl and Nusselt numbers. By interpolation from published data (Refs. 12 and 13) these values are

$$c_p = 5.9 \text{ kJ/kg K},$$
$$\mu = 0.188 \text{ g/ms},$$
$$\rho = 33 \text{ g/m}^3,$$
$$\kappa = 3.15 \text{ W/Km},$$

then Re = 340, Pr = 0.353.

Thus $Nu = 0.78Re^{0.5} Pr^{0.33} = 10.2$ and since δH = 26.5 MJ/kg

$$P_{cv} = A \kappa Nu \delta H/dc_p$$
$$= 2706 \text{ W or } 2.71 \text{ kW}.$$

Power Transfer by Convection to the Wall of the Keyhole — The variation of heat transfer coefficient along the keyhole, induced by the increasing gas velocity, can be incorporated in an overall coefficient by integration over the length of the keyhole. For this it is necessary to assume a constant mass flow throughout the keyhole.

The heat transfer over a short section δx (Fig. 4) can be expressed in terms of the analysis describing the heat transfer to a plane surface from a parallel flow. Rogers & Mayhew (Ref. 8) present an analysis which describes the variation of local heat transfer coefficient, with distance from the leading edge of a flat plate up to the transition point between laminar and turbulent flow. McAdams (Ref. 14) and Kutaleladze (Ref. 15) suggest that such an analysis can be applied to flow over curved surfaces, such as analysis can be applied to

flow over curved surfaces, such as turbine blades, short nozzles, etc.

Then $P(\delta x)=(\kappa\delta H/c_p)\,(A\delta x/s)\,Nu(\delta x)$

It may be shown that, after integration,

$$P_{total} = D\,A_c\,\kappa\delta H\,Nu\,(L)/Lc_p$$

where A_c is the surface area of the curved sides of the cone

$$A_c = \pi\,[(d_o + d_L)/2]\,[L^2 + (d_o - d_L)^2/4]^{1/2}$$

and Nu(L) is the Nusselt number at x = L when

$$D = 4(\cos\theta)^{1/2} d_L/(d_o + d_L) = [4d_L/(d_o + d_L)]\,[L/(L^2 + (d_o - d_L)^2/L)^{1/2}]^{1/2}.$$

By inspection it can be seen that in the special case of a tube ($d_o = d_L = d$), D = 2, $A_c = \pi dL = A_t$ and $P_{total} = 2\,A_t\,\kappa\delta H\,Nu\,(L)/Lc_p$.

With a keyhole of dimensions considered here it can be shown by substitution that $\cos\theta = 0.949$ and D = 0.974 so that $P_{total} = 0.974 \times 2.43 = 2.37$ kW.

However, this analysis still does not take into account the enhancement of the heat transfer process by the component of the gas velocity which is normal to the walls of the keyhole. Stagnation point heat transfer calculations may, therefore, be made for the vertically projected area of the keyhole, i.e., $\pi(d_L^2 - d_o^2)/4$. We should also consider that the stagnation point will be at some point into the keyhole so that the velocity to be used should be for a position say at 5 mm diameter. For this particular keyhole the velocity, therefore, would be $323 \times 6^2/5^2$ assuming that m′ is still constant, i.e., v(5 mm) = 465 m/s. It can be shown that there is an additional contribution or enhancement of 708 W.

Therefore total convective heat transfer to the keyhole is

2.37 + 0.71 kW = 3.08 kW

Total Power Input to the Workpiece

The total power input to the weld (P_a) is given by

$$P_a = P_{el.} + P_{cv} + P_{r,w}\ .$$

Hence for the weld pool with no keyhole

$$P_a = 1.57 + 2.71 + 1.74 = 6.02\ kW$$

which gives a process efficiency of some 60% relative to the total power input to the arc (10 kW).

Similarly for the fully penetrated weld with a keyhole (assuming that $P_{el.}$ would be the same)

$$P_a = 1.57 + 3.08 + 1.92 = 6.57\ kW$$

which gives an efficiency of 66%.

Discussion and Conclusions

It has been shown that in a 10 kW plasma welding arc an efficiency of heat transfer to the anode of 60 to 66% is to be expected. Arata and Maruo (Ref. 16) claimed experimentally to have efficiencies in the range 50 to 75% within which the present predictions fit easily. Other experimental work (Ref. 6) puts the anode heat transfer efficiency as 53 to 60% which is in near agreement with the calculations made here.

Comparing these plasma arc results with those for gas tungsten-arc welding (Fig. 5) shows that the anode effects, which before contributed 39% of the total and 89% of the transferred power, now only contribute 16% of the total power and 24 to 26% of the transferred power. Convection has taken over as one of the dominant mechanisms with radiation also an important, and not yet properly quantified, parameter. The emissivity of the arc must be assessed before a more precise evaluation of the radiation contribution can be made. Here an assumed value for emissivity has been used, deduced from the overall radiation losses suggested by the Welding Handbook (Ref. 2).

References

1. Quigley, M. B. C., Richards, P. H., Swift-Hook, D. T., and Gick, A. E. F., *J. Phys. D.,* Vol. 6, 1973, pp 2250-2259.
2. *Welding Handbook,* 6th ed., Section 1, Chap. 2, American Welding Society, Miami, p 3.22.
3. Olsen, H. N., *Physics of Fluids,* Vol. 2, Chap. 6, 1959, pp 614-623.
4. Milner, D. R., Salter, G. R., and Wilkinson, J. B., *British Welding Journal,* Vol. 7, 1960, pp 73-88.
5. Gick and Quigley, private communication, 1974.
6. Tsuchiya, K., Indow, H., Matsunaga, T., and Nakano, E., *IIW Doc. 70-112,* 1970.
7. Emmons, H. W., *Modern Developments in Heat Transfer,* Ed. Ibele, W. Academic Press, 1963.
8. Rogers, G. F. C. and Mayhew, Y. R., *Engineering Thermodynamics Work and Heat Transfer,* Chap. 21, Longmans, 1964.
9. Eckert, E. R. G. and Pfender, E., *Welding Journal,* Vol. 46 (10), Oct. 1967, Res. Supp. 471-s to 480-s.
10. Wilkinson, J. B. and Milner, D. R., *British Welding Journal,* Vol. 7, 1960, pp 115-128.
11. Schoeck, P. A., "An Investigation of the Anode Energy Balance of High Intensity Arcs in Argon," *Modern Developments in Heat Transfer,* Ed. Ibele, W. Academic Press, 1963.
12. Drellishek, K. S., Knopp, C. F., and Cambel, A. B., *Report No. NU-GDL A.3.62,* 1962, Northwestern U., Illinois.
13. Lancaster, private communication, 1974.
14. McAdams, W. H., *Heat Transmission,* Chap. 9, McGraw-Hill, 1954.
15. Kutaleladze, S. S., *Fundamentals of Heat Transfer,* Chap. 11, Edward Arnold, 1963.
16. Arata, Y. and Maruo, H., *Trans. JWRI,* Vol. 1,1, 1972, pp 1-9.

WRC Bulletin 201 December 1974

1. "The Submerged Arc Weld in HSLA Line Pipe — A State-of-the-Art Review"
by P. A. Tichauer

The submerged arc weld in HSLA line pipe is examined by briefly reviewing the metallurgy of high-strength low-alloy steels and then considering how the welding process affects this metallurgy. Particular emphasis is given to the influence of thermo-mechanical processing and to the role of micro-alloy additions as they relate to strength, grain size and toughness. The metallurgy of the weld is contrasted to that of the base plate, and some recent investigations are reviewed. The influence of consumable selection is considered, and some recommendations for further study are made.

2. "Experience in the Development and Welding of Large-Diameter Pipes"
by M. Civallero, C. Parrini and G. Salmoni

The production of X70 pipes up to 30 mm wall thickness with high base-material toughness has become necessary and possible today. In the choice of the most suitable type of steel, the mill and field weldability problems have been considered, as well as the weld-joint toughness requirements.

Of the experimental solutions, the best appears to be a control-rolled dispersoid steel, with extra-fine structure (mostly acicular type) with reduced pearlite and controlled inclusions. This steel, welded with the normal double-pass submerged arc techniques, allows one to achieve good toughness in the heat-affected zone, and to improve weldability compared to conventional steels. By further improving the type of flux on the basis of the theories developed, and by widening the knowledge of the effects of chemical composition (correlation between chemical composition, liquid-and-solid, austenite-to-ferrite transformation and final structures), it is believed possible to improve the low-temperature toughness up to the 10 kg/cm^2 level at temperatures down to -40 C, in wall thicknesses up to 30 mm.

3. "New Development in Weldability and Welding Technique for Arctic-Grade Line Pipe"
by E. Miyoshi, Y. Ito, H. Iwanaga and T. Yamura

In this study, low-temperature burst tests were performed on 48-in. diameter × 1-in. thick × 8-ft long line-pipe specimens of a 1% Ni steel recently developed and produced by controlled rolling. Notches twice the size of the largest allowable defect in API Std. 1104 were incorporated in the longitudinal weld seam. Test data were assessed by a COD approach. Two heat inputs were used in welding the specimens. A special GMA welding technique was developed for the lower heat input. It was found that the lower heat input was the best method of improving the fracture toughness of the weld.

4. "Technology of Wires and Electrodes for Welding High-Strength Pipe"
by J. Grosse-Wordemann

During the past few years, developments have led to steel grades with improved mechanical properties and reduced carbon content, compared to the previously known carbon-manganese grades. The new steels have improved weldability and API grades X60, X65 and X70 are already in use. The development of X80 is close to completion. This paper reviews the latest technology in developing suitable filler metals for welding these high-strength line-pipe steels.

5. "Preliminary Evaluation of Laser Welding of X-80 Arctic Pipeline Steel"
by E. M. Breinan and C. M. Banas

Single- and dual-pass laser welds were made in an alloy steel currently being evaluated for potential Arctic gas pipeline applications. The laser welds exhibited excellent overall mechanical properties and a Charpy shelf energy greater than 264 ft-lb, which is substantially above that of the base material. Dual-pass welds exhibited a ductile-to-brittle transition temperature below -60 F. Increased shelf energy was attributed to a reduction in the visible inclusion content of the fusion zone while transition temperature was shown to be strongly dependent upon fusion-zone grain size.

Paper (1) was prepared for the Subcommittee on Line-Pipe Steels of the Weldability (Metallurgical) Committee of the Welding Research Council. The other four papers were presented at a session sponsored by this subcommittee during the 1974 AWS Annual Meeting.

The price of WRC Bulletin 201 is $8.00 per copy. Orders should be sent with payment to the Welding Research Council, 345 East 47th St., New York, N.Y. 10017.